2015 Euromicro Conference on Digital System Design

Estimation of Blood Pressure and Pulse Transit Time Using Your Smartphone

Alair Dias Junior*†, Srinivasan Murali‡, Francisco Rincon‡ and David Atienza*

*Embedded Systems Laboratory (ESL), EPFL, Switzerland.
E-mail: david.atienza@epfl.ch
†FUMEC University, Brazil.
E-mail: alair.djr@fumec.br
‡SmartCardia GmbH, Switzerland.
Email: {srinivasan.murali, francisco.rincon}@smartcardia.com

***Abstract*—It is widely recognized today that there is an alarming rise of lifestyle-induced chronic diseases (e.g., type II diabetes) in our society. Therefore, a strong need exists for cost-effective and non-invasive devices that can measure blood pressure (BP) to monitor, diagnose and follow-up patients at risk, but also healthy population in general. One promising method for arterial BP estimation is to measure a surrogate marker of it, such as, Pulse Transit Time (PTT) and derive pressure values from it. However, current methods for measuring PTT require complex sensing and analysis circuitry and the related medical devices are expensive and inconvenient for the user to wear.**
In this paper, we present a new smartphone-based method to estimate PTT reliably and subsequently BP from the baseline sensors on smartphones. This new approach involves determining PTT by simultaneously measuring the time the blood leaves the heart, by recording the heart sound using the standard microphone of the phone and the time it reaches the finger, by measuring the pulse wave using the phone's camera. Moreover, we also describe algorithms that can be executed directly on current smartphones to obtain clean and robust heart sound signals and to extract the pulse wave characteristics using smartphones. We also present methods to ensure a synchronous capture of the waveforms, which is essential to obtain reliable PTT values with inexpensive sensors. Our experiments show that the computational overhead of the proposed two-phase processing method is minimum, with the ability to reliably measure the PTT values in a fully accurate (beat-to-beat) fashion using directly state-of-the-art smartphones as medical devices.

I. Introduction and Related Work

Our modern society is today threatened by an incipient health care delivery crisis caused by the current demographic and lifestyle trends. As a matter of fact, according to the World Health Organization (WHO), cardiovascular diseases (CVD) account for one third of the total deaths in the world. More than 50% of CVD related deaths arise from complications of hypertension and 40% of adults aged 25 and above were diagnosed with hypertension worldwide in 2008 [1]. In this endemic scenario, prevention and early diagnosis are key to reduce the economic and social costs related to hypertension.

This work has been partially supported by the Brazilian agency CAPES (grant no. 2171-13-9), and by the ObeSense (no. 20NA21_143081) RTD project evaluated by the Swiss NSF and funded by Nano-Tera.ch with Swiss Confederation financing.

During the last decades, ambulatory measurement of arterial blood pressure (BP) has been prescribed to patients suspected to suffer from hypertension [2] in an attempt to mitigate the problem. Current devices for non-invasive measurement of blood pressure (NIBP), nevertheless, are cumbersome equipments based on mechanical or oscillometric recordings and require a pressure cuff to be placed on the patient's upper arm or wrist. The periodic inflation of the cuff, usually every 20 minutes, is uncomfortable and noisy, disturbing the patient sleep and interfering with the BP measures themselves. Moreover, those devices cannot be used to obtain continuous beat-to-beat recording of BP changes, as they require a gap of 2-3 minutes between subsequent recordings. It is, therefore, clear that there is a strong need for new NIBP methods to monitor, diagnose and follow-up patients at risk, as well as for healthy people for early diagnosis.

Several recent works have presented novel ways of measuring BP using different sensors [3], [4], [2], [5], [6], [7], [8], [9]. The most promising ones measure the pulse transit time (PTT) differences between different waveforms, such as the electrocardiogram (ECG), photo-plethysmogram (PPG), phonocardiogram (PCG), impedance cardiogram (ICG), electrical impedance tomography (EIT) or a combination of them. In fact, the use of PTT to derive BP variations has been explored over the last several decades. For example, the Casio BP-100 [10] was a pioneering consumer watch that could measure pulse and ECG (by touching the watch from the other hand) and derive the PTT based BP variations.

In [2] a chest sensor is proposed to assess PTT based on ECG, PPG, and ICG. In all the cases, the underlying principle is that arterial stiffness increases with BP in a predictable manner, also affecting the pulse wave velocity (PWV) along the arterial tree. Hence, by measuring the time the pulse wave takes to travel from one point of the arterial tree to another, it is possible to calculate the PWV and estimate BP using elasticity based models of the blood vessels.

Nonetheless, recent research has shown that reliable BP measurements with PTT based methods require, at least, an initial calibration to model the individual PTTxBP relationship [3], or even a periodic calibration process to compensate for intra-patient variations, specially due to the vasomotion

978-1-4673-8035-5/15 $31.00 © 2015 IEEE
DOI 10.1109/DSD.2015.90

phenomenon. Hence, a standard BP measurement device based on mechanical or oscillometric recordings is used during the calibration step to feed the model with the required parameters. In particular, [5] details a system to estimate BP at the femoral artery using an ECG and a PPG sensor placed on the patient's thumb to calculate PTT. The system includes a brachial pressure cuff to perform periodic calibrations (every 4-8 hours) to compensate for inter and intra-patient variations of the PTTxBP relationship, which shows the feasibility of meeting FDA standards for medical grade devices.

Alternatively, research on the calibration step using different points of the patient is presented in [8], where BP monitor consisting of twin in-line PPG sensors that measure the pulse arrival time (PAT) using the wrist and little finger is described. Then, PTT is calculated by subtracting one PAT from another. The calibration procedure is performed by a set of wrist movements that change the external pressure applied by a band placed on the patient's wrist, but the results do not assess the precision of the calibration procedure. Similarly, [11] proposes the use of hydrostatic pressure changes, but no consistent experimental results have validated this approach so far. Also, [4] uses smartphones to measure PTT and estimate differential blood pressure using two different setups. The first one uses two smartphones synchronized via a self-designed bluetooth synchronization protocol. One device records the PPG using the camera while the other is used to record the sounds from the heart. Due to this synchronization procedure, the smartphones must be rooted (i.e., user applications needs to be given permission to run privileged commands), replacing their stock configuration. The second setup uses one smartphone and a customized external microphone to record heart sounds, which outlines the capabilities of smartphones sensors for PTT measurements. However, methods are still missing to perform reliable PTT calibration in wearable devices for BP estimation.

Beyond the concern on calibration methodologies for PTT, the reality is that a large set of works have evaluated the use of PTT as a surrogate marker for BP. We refer the interested reader to Henning and Patzak [12], which provides a complete summary of most of the relevant works, and comes to the conclusion that PTT is suitable for continuous monitoring of BP. The authors state that previous works results are encouraging enough for further clinical evaluation of PTT-based BP measurement methods. However, the major challenge of using PTT to estimate BP is the high degree of exactness and precision required in the acquisition and delineation steps. Usually, this is achieved by using expensive high-precision sensors and heavy signal processing techniques. However, to deliver an ambulatory solution for continuous NIBP measurements, low cost and ease of use are key factors.

In this work we describe new on-board methods to obtain clean and robust heart sound signals and to extract the pulse wave characteristics using just baseline sensors of smartphones with stock configuration. We also present methods to ensure a synchronous capture of the waveforms, which is essential to obtain reliable PTT values with inexpensive sensors. The rest of the paper is structure as follows. In Section II we present the overview of the proposed solution and how all the subsystems work together. Then, Section III describes in detail the signal acquisition and processing steps for both PPG and PCG recordings. Experimental results are presented next in section IV followed by the conclusions in Section V.

II. Background and Method Overview

PTT calculation involves the acquisition of the pulse arrival time (PAT) at two different points of the arterial three. Once the PATs are computed, the PTT can be calculated by the formula presented in equation 1.

$$\mathrm{PTT} = \mathrm{PAT}_1 - \mathrm{PAT}_0 \tag{1}$$

The first point on the arterial tree, which corresponds to PAT_0, is usually called proximal point, and the point used to determine PAT_1 is called distal point. The method we describe in this section uses the smartphone's internal microphone and camera to reliably compute the PATs at the proximal and distal point, respectively, and then estimate BP.

Differently from most of the previous works, here PAT_0 is computed from the heart sounds instead of the R-peak of the ECG wave. During the cardiac cycle, vibrations caused by the heart mechanical activity propagate through the chest, originating sounds that physicians have been using for centuries to assess the health of the heart. At least two heart sounds are very discernible on a healthy person. These sound events are usually referred as S1 and S2. S1 is believed to include four major components [13]: 1) The initial contraction of ventricles, which increases the ventricular pressure and accelerates the blood towards the atria; 2) The momentum of the moving blood as it forces the closure of the atrioventricular valves; 3) The oscillation of blood during the opening of aortic and pulmonary valves; and 4) The turbulence caused by the blood flowing through the Aorta. On the other hand, S2 includes two components that signals the closing of aortic and pulmonary valves. Figure 1 shows a representation of the heart sounds S1 and S2 and their major components.

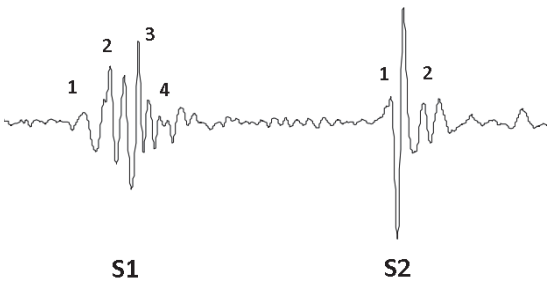

Fig. 1. Heart Sounds S1 and S2. Adapted from [13].

We are particularly interested in detecting the moment the blood leaves the heart as this is the genesis of the pulse pressure wave. This instant is marked by the third and forth components of S1 and, by correctly delineating S1, it is possible to precisely compute PAT_0. We use the smartphone's internal microphone as a low cost phonocardiogram to perform this task, thus computing the PAT at the proximal point.

The PAT at the distal point is computed using the smartphone's camera as a photo-plethysmogram (PPG) sensor. PPG is a non-invasive method that uses optics to obtain information about the subcutaneous blood circulation [2]. PPG sensors

gather the light transmitted through the living tissue and use the acquired signal to estimate arterial pulsatility and blood content. Our method uses the smartphone's flash light and camera to mimic a skin reflectance based [14] PPG sensor. During the measurement, the subject holds his/her index fingertip over both the camera and the flash light. The light emitted by the LED is scattered by the living tissue, reflected by the digital phalange, and finally captured by the camera. The subtle changes in brightness due to the blood flow are used to reconstruct the blood pulse-wave signal. All signal acquisition, processing and delineation of the waveforms are performed in real-time to provide the user with visual and audio feedback. During the experiments we noticed that this feedback is essential to help the user to position the sensors, specially the microphone, at the right place. Moreover, audio-visual feedback enriches user experience, making the application more interactive and appealing.

This real-time feedback, nevertheless, puts an extra burden on the signal processing algorithms. To provide for a smooth execution during the real-time processing without negatively affecting the system robustness, we have split the signal processing step in two phases. Phase I performs a simple conventional filtering of the signals and a coarse delineation of the waveforms. This phase has two objectives: 1) extracting a clean signal with quality enough to be presented to the user; and 2) checking if the recorded signals have enough quality to be delineated in the second phase. During Phase I we just perform a preliminary analysis of the signals, not ensuring a perfect synchronization between the waveforms neither a precise delineation of their fiducial points.

The filtered samples are accumulated in a circular buffer during Phase I to be processed in the second phase. Once the required signal quality is met, the algorithms in Phase II further filter the signals, analysing the entire buffer using advanced signal processing techniques. These algorithms rely on the fact that PPG and PCG are time-locked, as they are triggered by the same bio-event: the pumping of the heart. This multi-modal approach grants a robust and reliable delineation of the waveforms even using the inexpensive sensors present in stock smartphones. In Phase II, the precise fiducial points of the waveforms are detected and used to calculate PTT.

After computing the PTT, its value is fed to the blood pressure estimation model. Before starting using the application, the user must calibrate the model using a standard BP device, like the oscillometric based devices largely available for ambulatory use. The calibration procedure requires the user to perform a PTT measurement using the smartphone. After the recording is done, the application asks the user to input a reference BP value collected with an standard BP device. The BP reference value is used to calibrate the PTTxBP model.

We employ a multi-point adaptive calibration method, which requires at least two points with different BP values to model the PTTxBP relationship. This method compensates for changes in the user specific PTTxBP relationship by evaluating and discarding previous calibration points as soon as they are not valid. Every time the user calibrate the system, a new point is added to the curve fitting algorithms and the previous points are evaluated to be discarded. With this approach, the more the user calibrates the model, the more precise it becomes. However, even with just a few calibration points, the provided results are reliably enough to track BP changes.

III. Smartphone Based Signal Acquisition and Processing

Enabling cost-effective health care based services on the mobile phones is the next step on telehealth systems. People are used to take their mobile phones everywhere, keeping them all day long in reach of their hands. This ubiquity make mobile phones perfect to follow-up patients at risk and to monitor sporadic vital signs deviations from the baseline. The biggest challenge, however, is how to deliver an effective health care solution using mobile phones without impacting neither the battery life nor the user experience due to the limited processing capabilities.

In this section we detail the acquisition and processing of PPG and PCG using the smartphones' baseline sensors. We focus on the Android operating system as it detained 82% of the market share in 2014 [15]. Most of the techniques presented here, nevertheless, are generic enough to be applied to other operating systems with little to no modification.

A. Photo-plethysmography Acquisition

The proposed system uses the smartphone's camera as a PPG sensor to monitor the pulse waveform. Other mobile applications use the same principle to measure the subject's heart rate (HR), like the Azumio's Instant Heart Rate app [16]. Usually, the PPG signal is reconstructed from the individual frames of the camera and fed to a Fast Fourier Transform (FFT) algorithm that extracts the HR value. Frequency domain analysis, like FFT, may be robust enough to extract HR, but it is not sufficient for PTT calculation. In order to estimate blood pressure, we need to detect the exact moment the pressure pulse reaches the distal point (i.e. the fingertip), which requires the PPG signal to be precisely reconstructed and delineated in the time domain.

A major problem for PPG reconstruction arises when standard smartphones are used to capture the signal, specially Android based ones. There is little hardware standardization among Android devices and the operating system lacks of support for frame temporization. Constant frame rates are not supported by the vast majority of devices and, as a consequence, the PPG reconstruction and delineation algorithm must take into account variable frame rates, specially those due to automatic exposure adjustment, and to restricted processing capabilities.

Automatic exposure (AE) allows the smartphone's camera to automatically determine the correct exposure time for compensating for poor lighting during recordings. Despite desirable in normal use, this feature may distort the PPG signal when the pulse waveform is being acquired. Dynamic adjustment of exposure has two effects on the recorded PPG signal: 1) it changes the frame rate during the acquisition, distorting the signal time reference; and 2) it constantly changes the image brightness, distorting the amplitude of the signal. Hence, to get a non-distorted PPG signal, which is essential to correctly determining the fiducial points, the exposure time must be locked during the recordings.

We adopted a solution to prevent the AE feature to affect the measurements. After the user covers the lens to start the measure, we allow the AE feature to adjust the exposure for a few seconds and, then, lock the exposure to get a clean signal thereafter.

With respect to the restricted processing capablilities, we used a frame buffer to guarantee that no frames are dropped by the operating systems during the demanding tasks and adopted a thread based solution to take advantage of the multicore architectures whilest also preventing the user interface from hanging while during the computations. The PPG value is therefore computed frame by frame by a handler thread, using the mean brightness in the red channel of the image. This value is then passed to the phase I algorithms for filtering and coarse delineation.

B. Phonocardiogram Acquisition

Differently from the camera, Android audio recordings have a constant sample rate, which is set via software before starting the acquisition. We use a sample rate of 44100 Hz as, according to the *Android 4.4 Compatibility Definition* [17], this is currently the only sample rate guaranteed to work on all devices. However, we downsample the recording to 900 Hz before processing to reduce the required amount of computation. To guarantee we receive the raw samples from the microphone, we disabled the device's automatic gain control and noise reduction features.

PCG acquisition in Android systems, nevertheless, is not at all issue-free. First, all read operations involving the audio device are blocking and, hence, a working thread must be set up to prevent the system from hanging during recordings. Last, but not least, the Android's compatibility document only suggests that the hardware manufacturers reduce the audio latency, but does not require them to do it. Again, according to the *Android 4.4 Compatibility Definition* [17], the latency to get the first audio sample *should* be lower than 100 ms while in the rest of the recording, latency *should* be lower than 45 ms. These latency figures are just recommendations, not mandatory.

To circumvent the latency problem (and also to control the number of samples in the circular buffer during the first phase of the signal processing) we mark each sample with a timestamp that is relative to the moment the sampling started, not the moment we start to receive the samples. The premise of this solution is that the sample rate of the audio channel is constant and the latency happens just for delivering the audio data, not for the hardware to start sampling. By doing this, we were able to achieve sufficient synchronization between audio samples and video frames to calculate the PTT reliably.

C. Phase I

As previously stated, the first objective of Phase I is to extract a clean signal, with quality enough to be presented to the user. Thus, during this first phase, the PPG and PCG input samples are filtered before storing them in a circular buffer. Filtering the acquired signals is fundamental for correctly extracting their fiducial points. However, filtering usually incurs in a phase difference between the input and output signals. Sometimes, the filter phase response is non-linear (the phase shift is not directly proportional to the frequency) which may result in distortions that have an impact on the accuracy of the fiducial points detection. Here, we use two types of digital filters: Finite Impulse Response (FIR) and Infinite Impulse Response (IIR) [18]. In the case of linear phase FIR filters, the phase difference from the input signal can be easily compensated by subtracting a constant value from the sample timestamp. IIR filters, on the other hand, usually have non-linear phase response, which causes distortions in the signal. However, IIR filters are computationally more efficient then FIR filters which is a significant advantage when processing capability is restricted.

TABLE I. FILTERS SPECIFICATIONS

Name	Type	Order	Sample Frequency (Hz)	Cut Low (Hz)	Cut High (Hz)
PPG Signal	Bandpass IIR	6	30	0.5	20
PCG Downsampling	Lowpass FIR	559	44100	450	•
PCG Signal	Bandpass IIR	2	900	20	250
PCG Envelope	Lowpass IIR	2	900	20	•

We opted to use IIR filters whenever possible to reduce the processing requirements of the system. The distortions caused by the phase non-linearity do not have significant impact on the user feedback and, hence no effort was made to eliminate them during Phase I. In Phase II, nevertheless, the distortions may affect the PTT calculation and then we use techniques that sacrifice the real-time processing for linearity, as it will be presented in the next subsection. Table I shows the design parameters for the filters used in phase I and phase II. All filters were designed using Matlab's filter toolbox [19].

Two circular buffers were defined for storing the values of each bio-signal (two for PPG and two for PCG). The first buffer (*view buffer*) holds the data that will be presented to the user in real-time during Phase I. The second buffer (*data buffer*) contains the data used to calculate PTT in phase II. This separation between *view* and *data* buffers improves the real-time data processing, since the data presented to the user does not require to be precise, but just representative enough to give the user a quality feedback. The real-time processing over the *view buffer* is efficient specially because of two factors:

1) the *view buffer* is smaller than the *data buffer*, since just a few heart cycles are sufficient to provide the user with audio-visual feedback;
2) all filtering, except for the *PCG Downsampling*, is performed by causal IIR filters, since light distortions in the user feedback do not interfere with usability.

Every time a new PPG sample is calculated from the camera frames, a pair <*value, timestamp*> is inserted into the PPG *data* and *view* buffers. The value added to the *data buffer* is inserted without any filtering or processing, while the value inserted into the *view buffer* is filtered using the *PPG Signal* filter presented in table I. Since it is an IIR filter, the data will be lightly distorted, but without impacting the PTT calculation, which uses the *data buffer* in Phase II.

```
1  FUNCTION Phase_I
2    TRIGGER: A new sample is inserted into
3             the PPG buffer
4  BEGIN
5    if (PPG dataBuffer is full) then
6      align PPG and PCG data buffers
7      delineate PPG view buffer
8      if (PPG delineation is good enough) then
9        delineate PCG view buffer guided by PPG
10       if (PCG delineation is good enough) then
11         call Phase_II
12       endif
13     endif
14   endif
15 END
```

Listing 1. Phase I Algorithm

The samples from the audio device, on the other hand, are downsampled in real-time using the *PCG Downsampling* filter before being inserted into the buffers. The *PCG Downsampling* filter has a linear phase and downsamples the audio signal from 44100 Hz to 900 Hz, while also works as a lowpass filter, attenuating components above the Nyquist Frequency at the same time. Before being inserted into the *view buffer*, the PCG samples are further processed to create an envelope that allows the user to identify the heart sounds S1 and S2. First, the *view* samples are filtered by the *PCG Signal* filter. Then, the samples are normalized to the interval $[0.00, 1.00]$ and used to calculate the energy, using the formula presented in equation 2. Finally, the samples are filtered using the *PCG Envelope* filter, which creates an envelope of the signal.

$$E(t) = -x(t)^2 . \log(x(t)^2) \tag{2}$$

Where $E(t)$ is the energy at time t and $x(t)$ is the filtered sample value at time t.

Besides filtering and inserting data into the buffers, Phase I also coarsely delineates and analyzes the signals to trigger the execution of Phase II algorithms. Listing 1 presents a high level algorithm for this task.

PCG data acquisition is performed precisely at 44100 Hz and the signal is downsampled to 900 Hz before inserting into the circular *data* and *view* buffers. The PCG *data buffer* was designed to hold 14 seconds of samples while the *view buffer* is capable of storing 4 seconds. Once filled, the buffers start discarding the oldest samples every time a new sample is inserted. PPG, on the other hand, has a variable frame rate and automatic sample discarding based on the number of samples is not possible. Hence, before analysing the signals, PPG and PCG buffers must be synchronized. This task is performed by the alignment proceedure, executed at line 6 of Listing 1. Since the sample rate of PCG is much higher than that of PPG, the synchronization is performed by getting the first timestamp from the beginning of the PPG buffer and discarding all data that precedes it in the PCG buffer.

After aligning the PPG and PCG buffers, the PPG signal stored in the *view buffer* is delineated (line 7 of Listing 1). The objective of the delineation phase is to detect the moment the pulse wave reaches the finger. This moment is marked by the onset of the PPG pulse waveform and is determined using the following steps:

1) the minima of the waveform are detected using the derivative of the signal;
2) the detected minima, so-called feet, are analysed according to their amplitudes. All points that do not fall into the valid range (that are determined experimentally) are discarded;
3) the time difference between two given feet is checked for significant deviations from the mean. If two feet are too close from each other, their neighbours are checked, trying to solve these discrepancies. If removing one of them solves the deviation, that foot is discarded;
4) the remaining points are checked for zero-crossing points between them. All PPG wave feet must be separated by two zero-crossing points. If this condition is not met for any given two feet, the one with lower amplitude is kept and the other one is discarded.

Once the feet of the pulse waves are detected, they are checked for stability (line 8 of Listing 1). If the longest beat is greater than 1.5 times the shortest beat, probably the delineation algorithm missed one beat or wrongly detected a pulse wave onset. Otherwise, the detected points time difference is stable and the PPG delineation is considered good enough.

The next step is to delineate the PCG signal (line 9 of Listing 1). PCG signal is significantly more difficult to be delineated than the PPG because of the noise captured by the smartphone's microphone. However, the complexity of this task is attenuated as we already have information regarding the individual heart beats, extracted during the PPG delineation. In a normal condition, an onset in the PPG signal must follow every S1 sound event in the PCG signal. For the coarse delineation executed in Phase I, we check for pairs of peaks in the PCG envelope (S1 and S2) that are way above the average signal value. If a pair of peaks within a valid time difference precedes each one of the PPG onsets, the PCG signal has enough quality to be processed and the second phase of the analysis is triggered.

D. Phase II

The algorithms in Phase II are very similar to the ones in Phase I except for the fact that they use the bigger *data buffers* instead of the *view buffers*. There are some important differences, nevertheless, that significantly improve the quality of delineation in the second phase.

First, the IIR filters are applied over the *data buffers* in both directions during Phase II, using a forward-backward scheme. This results in a non-causal filter that is realizable just because all samples have already been acquired and are stored in the buffers, ready to be processed. Using this technique, the result is a signal without the phase distortions that would impact on the fiducial points determination.

Second, we use a more robust technique to delineate the PPG and PCG signals. The technique is based on ensemble averaging the signals to remove noise that is unrelated to the heart beat. This technique rely on the fact that over short time windows, the PCG and PPG fiducial points may be considered

time-locked. Solà [2] used ensemble average (EA) to filter the ICG signal using ECG R-wave peaks as triggers. The author demonstrated that using EA corresponds to applying a very narrow band-pass filter with central frequencies defined by the heart rate frequency and its harmonics. Here we calculate the EA using the onsets of the PPG signal as trigger points, since this signal is, in general, less noisy than the PCG.

Let τ_i be the timestamp of the ith onset of the PPG wave and N be the number of detected onsets during the PPG delineation of the *data buffer* in Phase II. The ensemble average of the signal, $\hat{s}$, is computed over the original signal, s, using the formula presented in equation 3.

$$\hat{s}(t) = \frac{1}{N}\sum_{i=1}^{N} s(t+\tau_i) \tag{3}$$

where $t \in [0, T)$ and T is the heart beat period. Figure 2 illustrates the computation of the ensemble average.

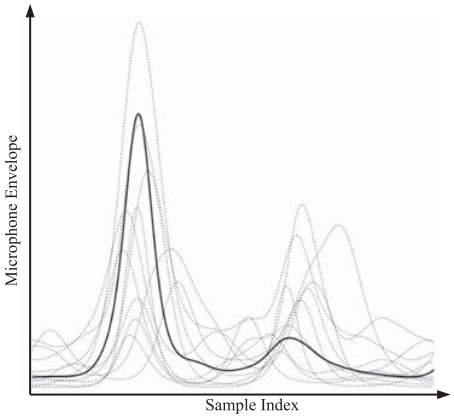

Fig. 2. PCG filtering using the Ensemble Average Technique

By computing $\hat{s}$ using equation 3, we obtain a denoised version of a single heart beat of s, averaged over N heart beats of that signal. After applying this technique over both the PPG and PCG, we have two options for calculating PTT:

1) delineate both $\hat{s}_{PPG}$ and $\hat{s}_{PCG}$ and calculate the PTT using the detected fiducial points;
2) use $\hat{s}_{PPG}$ and $\hat{s}_{PCG}$ as template waveforms to delineate the original signals, s_{PPG} and s_{PPG}, and calculate N PTTs for the N heart beats.

We use the first option when determining the instantaneous BP measurement. Using the PTT calculated from the ensemble averages of the signals, we obtain a more stable PTT that is robust to noise and to single beat deviations from the baseline value. On the other hand, option 2 is used to track beat-to-beat variations of BP, caused by special situations like standing up, or performing the Valsalva-Weber manoeuvre [20].

IV. Experiments

We performed a series of experiments to evaluate the proposed filtering and delineation algorithms. It is worth noting that the experiments are not intended to validate the use of PTT as a surrogate marker for blood pressure as this issue has been addressed by several previous works. We aim at validating our solution with respect to three major aspects: 1) the synchronization between PPG and PCG signals; 2) its capability of tracking beat-to-beat BP changes; and 3) the accuracy in determining the waveforms fiducial points.

Experiments were performed using a Samsung S4 smartphone running Android 4.4 operating system. Data was collected and processed using a hybrid application developed in Java and C. We opted to use C in the signal processing algorithms because native code libraries present better time performance than pure Java applications. Despite all results presented in this section were obtained using solely the mobile application, for convenience we used the software Matlab [19] to create the plottings.

A. Synchronization between PCG and PPG

As the PCG and PPG signals are acquired by different subsystems of the smartphone, it is necessary to check whether they are being generated in perfect synchronization. If the signals are not correctly aligned in time, the accuracy of the obtained PTT value would be compromised. A simple procedure was adopted to evaluate the synchronization between PCG and PPG: we applied a sequence of tappings on the smartphone, each tap completely covering the camera lenses and generating a sound at the same time. If data acquisition and synchronization are correctly performed by the application, the generated PPG and PCG waveforms should present a perturbation around the same time instant.

This experiment was performed several times to make sure fluctuations on the frame rate and other transitory conditions do not affect the synchronization between the signals. During its execution, we have noticed that the camera waveform peak always happened two frames before of the microphone peak. In order to synchronize both signals, we added a constant delay to the time-stamp of each camera sample. The result of the experiments, after this latency problem correction is presented in Figure 3. With this correction, the waveforms present perfect synchronization, therefore showing that the adopted synchronization scheme is suitable to reliably calculate PTT.

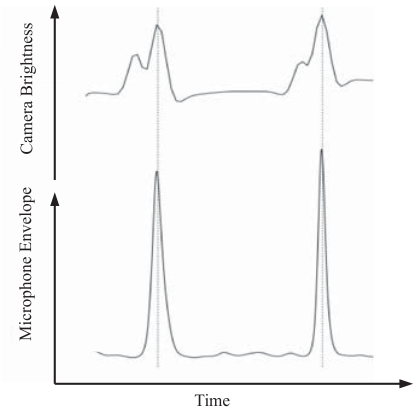

Fig. 3. Synchronization Experiment Results

B. Tracking of Beat-to-beat BP Changes

In order to evaluate the capability of the developed solution to track beat-to-beat variations of BP and HR, it is required that a disturb is induced on the user's cardiovascular system, thus generating observable changes on the monitored signals during the PCG and PPG acquisition. Usually, these changes in BP and HR are created by submitting the user to a series of physical exercises. However, the solution we propose in the present work is not suitable for use during physical activities as it requires the user to stand still or seat in a specific position, preferably on a quiet environment. The movement of the body, during the exercises would add too much noise on the PCG acquisition, specially due to the microphone-skin friction. Hence, we opted to employ the Valsalva-Weber maneuver to produce the changes on the monitored signals.

The Valsalva-Weber maneuver consists in asking the patient to perform a full inspiration followed by a sustained forced expiration against the closed glottis, nose, and mouth. After a few seconds, the expiration restraint is loosened and the patient should try to breath as normally as possible.

During the execution of Valsalva-Weber maneuver, it is possible to observe four phases in which acute changes in HR and BP occur [20], as depicted in Figure 4. During the initial inspiration (phase I), the HR shortly reduces and a sudden increase in systolic BP is perceived; As the subject maintain the expiratory strain (phase II), HR progressively increases, while Systolic BP decreases in a similar fashion; when breath is finally released (phase III), HR reaches its peak and BP fall shortly to its minimum level; the recovering phase (phase IV) is marked by a progressive reduction of HR, which reaches its minimum value before returning to the basal state. BP value also presents a progressive increase, with an overshoot before returning to pre-maneuver levels.

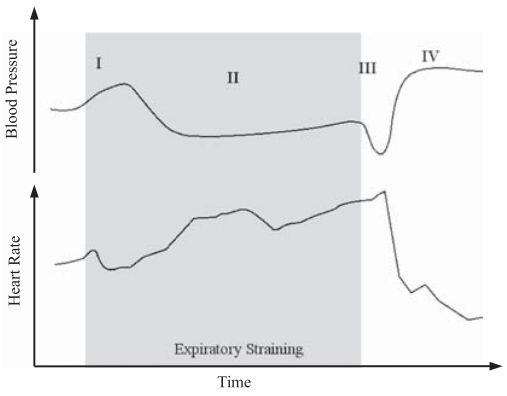

Fig. 4. Normal Behavior During the Valsalva-Weber Maneuver. Adapted from [20].

Three subjects were submitted to the Valsalva-Weber maneuver during the experiments: one female (subject 1) and two male (subjects 2 and 3). Subject 1 does not perform any regular physical activity, presenting a high basal HR of around 100 bpm. Subject 2 undergoes moderate physical activity twice a week, and Subject 3 is an active sportsman who performs intense training regularly. Figure 5 presents the waveforms for HR and relative (uncalibrated) BP for these subjects. Upon inspection of that figure, the four expected phases for both HR and BP curves are identified. The curves for the three subjects match the template of figure 4.

TABLE II. DIFFERENCE BETWEEN AUTOMATIC AND MANUAL DELINEATION

	PCG S1 (ms)		PPG Onset (ms)		PTT (ms)		
	Max	Mean	Max	Mean	Max	Mean	Mean Perc.
Subject 1	2.72	1.40	6.67	5.00	8.60	5.61	2.55%
Subject 2	5.49	2.27	13.30	5.14	11.76	5.19	2.04%
Subject 3	13.38	4.04	13.33	4.92	21.61	6.98	3.00%
Average	7.20	2.57	11.10	5.02	13.99	5.93	2.53%

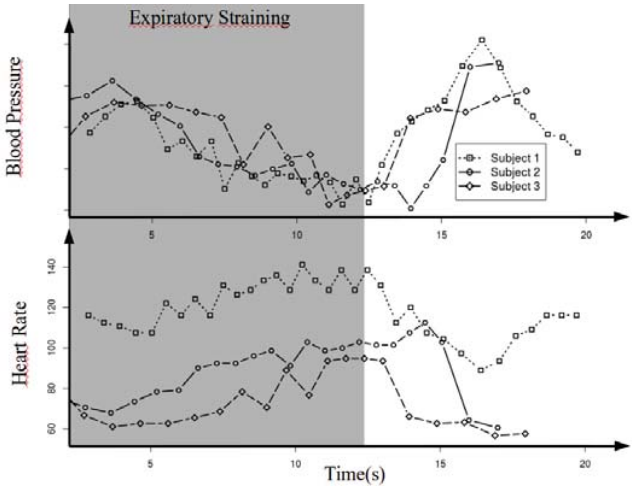

Fig. 5. Typical HR and BP Curve Obtained During the Experiments

C. Fiducial Points Classification Accuracy

We have also checked the delineation accuracy of the proposed methods. For the same three subjects for which the results were presented in section IV-B, PPG and PCG waveforms were delineated both automatically using the proposed algorithms, and manually by inspecting the raw waveforms before any processing. Manual PCG delineation was performed using the template waveform of figure 1 and, as previously stated, we used the third component of S1 as the proximal point. PPG manual delineation was performed using the intersecting tangent method [21] which defines the onset of the pulse wave as the intersection point between a tangent line through the initial systolic upstroke of the PPG waveform and a horizontal tangent line passing over the minimum point of the same wave. The maximum and mean difference between the manual and automatic determination of the points were recorded and the results are presented in table II.

During the compilation of table II data, we have noticed that Subject 2 was presenting a high maximum error for both PCG and PTT values. Upon careful inspection of the waveforms, we have found out that this high error figure was due to a misclassification during the manual analysis of the data. A spurious sound was captured by the microphone,

most probably due to an involuntary movement during the acquisition. This sound was mistaken during the manual PCG delineation by an S1 event and the subsequent peak, which was the real S1 peak, was assumed to be an S2 event. The automatic delineation algorithm, nevertheless, was able to correctly identify the actual S1 peak as it uses the PPG waveform and the time intervals to support the delineation. Figure 6 shows the misclassification and also the correct analysis of the waveform. After correcting this inspection, the manual delineation was corrected and the errors were recalculated.

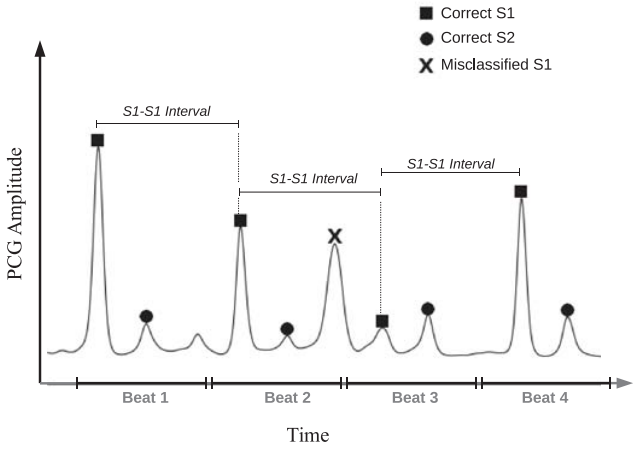

Fig. 6. Misclassification of Manual Delineation

V. Conclusion

In this paper, we have presented methods for reliable estimation of Pulse Transit Time, and hence Blood Pressure, using only mobile phones with stock configuration. The main contributions of the present research so far are: 1) a low profile two step processing method that supports real-time acquisition and processing of PCG and PPG waveforms, providing the user with audio-video feedback and enhancing his/her experience with the mobile application; and 2) a robust method for filtering PPG and PCG signals using the ensemble average technique to create a template waveform that is used to guide the delineation of the less-than-ideal signals acquired using inexpensive sensors. Besides these two main contributions, to the best of our knowledge, this is the first time short-term variations of BP are tracked beat-to-beat based solely on phono-cardiogram and photo-plethysmogram, both acquired using inexpensive sensing and analysis circuitry.

We have validated the solution across subjects using the Valsalva-Weber maneuver to induce acute beat-to-beat variations of BP and HR. The waveforms obtained during the experiments match the expected template for both signals (i.e., mean errors up to 3%). Thus, these results indicate that our proposed methods are reliable for ambulatory monitoring of short-term variations in blood pressure values using just current smartphone devices.

References

[1] World Health Organization, "A global brief on hypertension," World Health Organization, Geneva, Switzerland, Tech. Rep., 2013.

[2] J. M. Solà i Carós, "Continuous non-invasive blood pressure estimation," Ph.D. dissertation, ETH Zürich, 2011.

[3] J. Sola, M. Proenca, D. Ferrario, J.-A. Porchet, A. Falhi, O. Grossenbacher, Y. Allemann, S. Rimoldi, and C. Sartori, "Noninvasive and nonocclusive blood pressure estimation via a chest sensor," *Biomedical Engineering, IEEE Transactions on*, vol. 60, no. 12, pp. 3505–3513, Dec 2013.

[4] V. Chandrasekaran, R. Dantu, S. Jonnada, S. Thiyagaraja, and K. Subbu, "Cuffless differential blood pressure estimation using smart phones," *Biomedical Engineering, IEEE Transactions on*, vol. 60, no. 4, pp. 1080–1089, April 2013.

[5] M. Banet, M. Dhillon, and D. McCOMBIE, "Body-worn system for measuring continuous non-invasive blood pressure (cnibp)," Jun. 24 2010, uS Patent App. 12/650,383. [Online]. Available: http://www.google.com/patents/US20100160795

[6] R. Sethi and J. Watson, "Systems and methods for non-invasive blood pressure monitoring," Apr. 1 2010, wO Patent App. PCT/IB2009/006,136. [Online]. Available: http://www.google.com.ar/patents/WO2010001233A3?cl=en

[7] G. Kuchler, "Noninvasive blood pressure determination method and apparatus," May 20 2008, uS Patent 7,374,542. [Online]. Available: http://www.google.com.br/patents/US7374542

[8] D. McCombie, A. Reisner, and H. Asada, "Motion based adaptive calibration of pulse transit time measurements to arterial blood pressure for an autonomous, wearable blood pressure monitor," in *Engineering in Medicine and Biology Society, 2008. EMBS 2008. 30th Annual International Conference of the IEEE*, Aug 2008, pp. 989–992.

[9] P. Shaltis, A. Reisner, and H. Asada, "Wearable, cuff-less ppg-based blood pressure monitor with novel height sensor," in *Engineering in Medicine and Biology Society, 2006. EMBS '06. 28th Annual International Conference of the IEEE*, Aug 2006, pp. 908–911.

[10] L. CASIO COMPUTER CO., "Module no. 2196," 1993. [Online]. Available: http://ftp.casio.co.jp/pub/world_manual/wat/en/qw2196.pdf

[11] D. McCOMBIE, M. Dhillon, and M. Banet, "System for calibrating a ptt-based blood pressure measurement using arm height," Mar. 18 2014, uS Patent 8,672,854. [Online]. Available: http://www.google.com/patents/US8672854

[12] A. Hennig and A. Patzak, "Continuous blood pressure measurement using pulse transit time," *Somnologie - Schlafforschung und Schlafmedizin*, vol. 17, no. 2, pp. 104–110, 2013. [Online]. Available: http://dx.doi.org/10.1007/s11818-013-0617-x

[13] C. Ahlström, *Nonlinear phonocardiographic Signal Processing [Elektronisk resurs]*. Institutionen för medicinsk teknik, 2008.

[14] Y. Mendelson and B. Ochs, "Noninvasive pulse oximetry utilizing skin reflectance photoplethysmography," *Biomedical Engineering, IEEE Transactions on*, vol. 35, no. 10, pp. 798–805, Oct 1988.

[15] Gartner, Inc., "Gartner says sales of smartphones grew 20 percent in third quarter of 2014," Dec. 1 2014. [Online]. Available: http://www.gartner.com/newsroom/id/2944819

[16] Azumio Inc., "Instant heart rate by azumio," Mar. 2015. [Online]. Available: http://www.azumio.com/s/instantheartrate/index.html

[17] Google Inc, "Android 4.4 compatibility definition," Nov. 1 2013. [Online]. Available: http://static.googleusercontent.com/media/source.android.com/pt-BR//compatibility/4.4/android-4.4-cdd.pdf

[18] S. Haykin and B. Van Veen, *Signals and Systems*. John Wiley & Sons, 2002.

[19] MathWorks, Inc., "Matlab - the language of technical computing," Mar. 1 2015. [Online]. Available: http://www.mathworks.com/products/matlab/

[20] L. F. J. Jr., "Teaching cardiac autonomic function dynamics employing the valsalva (valsalva-weber) maneuver," *Advances in Physiology Education*, vol. 32, no. 1, pp. 100–106, 2008. [Online]. Available: http://advan.physiology.org/content/32/1/100

[21] Y. C. Chiu, P. W. Arand, S. G. Shroff, T. Feldman, and J. D. Carroll, "Determination of pulse wave velocities with computerized algorithms." *Am Heart J*, vol. 121, no. 5, pp. 1460–70, 1991. [Online]. Available: http://www.biomedsearch.com/nih/Determination-pulse-wave-velocities-with/2017978.html